J. Non-Newtonian Fluid Mech. 166 (2011) 73–92

Contents lists available at ScienceDirect

Journal of Non-Newtonian Fluid Mechanics

journal homepage: www.elsevier.com/locate/jnnfm

Perturbation solution of Poiseuille flow of a weakly compressible Oldroyd-B fluid

Kostas D. Housiadas [a,*], Georgios C. Georgiou [b]

[a] Department of Mathematics, University of the Aegean, Karlovassi, Samos 83200, Greece
[b] Department of Mathematics and Statistics, University of Cyprus, P.O. Box 20537, Nicosia, Cyprus

ARTICLE INFO

Article history:
Received 8 June 2010
Received in revised form 18 October 2010
Accepted 18 October 2010

Keywords:
Oldroyd-B fluid
Poiseuille flow
Compressibility
Perturbation solution
Normal stress difference
Flow curve

ABSTRACT

The isothermal, planar Poiseuille flow of a weakly compressible Oldroyd-B fluid is considered under the assumption that the density of the fluid obeys a linear equation of state. A perturbation analysis for all the primary flow variables is carried out with the isothermal compressibility serving as the perturbation parameter. The sequence of partial differential equations which results from the perturbation procedure is solved analytically up to second order. The effects of the compressibility parameter, the aspect ratio, and the Weissenberg number are discussed. In particular, it is demonstrated that compressibility has a significant effect on the transverse velocity and the first normal stress difference.

1. Introduction

The importance of compressibility in viscous and viscoelastic flows of polymer melts and other liquids has been emphasized in many studies in the past few decades. Such flows correspond to low values of the Mach number, which is defined as the ratio of the characteristic speed of the fluid to the speed of sound in the fluid; the incompressibility limit corresponds to zero Mach number. Compressibility becomes significant in flows where a sufficient amount of fluid is subject to high pressures, such as the extrusion process [1], injection blow moulding, jet cutting and liquid impact [2], or in flows involving relatively long tubes, such as waxy crude oil transport [3], or locally near sharp corners [4]. The stick-slip polymer extrusion instability is caused by the combined effects of compressibility and non-linear slip [1,5]. Georgiou and Crochet [6] pointed out that the incompressibility assumption may lead only to minor errors to the steady-state solutions but can significantly affect the flow dynamics. The numerical simulations of Taliadorou et al. [7] of the extrusion of strongly compressible Newtonian liquids revealed that compressibility may also lead to oscillatory steady-state free surfaces. Hatzikiriakos and Dealy [8] noted that, although the isothermal compressibility of molten polymers is very small, it can have a dramatic effect on the time required for the pressure to level off in a capillary flow experiment. Ranganathan et al. [9] presented time-dependent experimental capillary flow data for a high-density polyethylene using the multipass rheometer and showed that the experimentally observed pressure relaxation on cessation of the piston movement can be almost entirely attributed to the compressibility of the melt alone. More recently, Valério et al. [10] demonstrated that the incompressibility constraint creates singularities that lead to non-physical eigenvalues at infinity which poses severe difficulties on linear stability analyses.

Numerical simulations of weakly compressible flows have been reported for different fluids: Newtonian [6,7], generalized Newtonian fluids, such as the Carreau fluid [11–13], the Bingham plastic [3], and the Herschel–Bulkley fluid [14], and viscoelastic fluids, such as the Oldroyd-B fluid [15] and the Rolie Poly model [12]. Keshtiban et al. [15] presented a time-marching pressure-correction/Taylor–Galerkin finite element algorithm for solving low Mach number compressible viscoelastic flows and applied it to contraction flows of an Oldroyd-B fluid. The compressible Oldroyd-B model was also used by Brujan [16] in his study of bubble dynamics in a compressible viscoelastic fluid, and by Webster and co-workers in subsequent works dealing with numerical algorithms for solving low Mach number viscoelastic flows [2,17,18]. Much earlier, Edwards and Beris [19] proposed a modification of viscoelastic models in the presence of compressibility and applied it to the upper-convected Maxwell model. Matusu-Necasova et al. [20] studied the existence and uniqueness of stationary solutions for the equations modelling the steady flow of compressible viscoelastic fluids of the Oldroyd type in an exterior domain.

* Corresponding author.
E-mail address: housiada@aegean.gr (K.D. Housiadas).

0377-0257/$ – see front matter © 2010 Elsevier B.V. All rights reserved.
doi:10.1016/j.jnnfm.2010.10.007

In the present work we derive the second-order regular perturbation solution for the planar isothermal Poiseuille flow of a weakly compressible viscoelastic fluid which follows the Oldroyd-B model. This is a popular viscoelastic constitutive equation predicting constant shear viscosity and strain-hardening properties in extension. To our knowledge, this is the first perturbation analysis of compressible viscoelastic flow. The present work can be viewed as an extension of the recent work by Georgiou and co-workers [21,22], who obtained perturbation solutions for the planar, the round, and the annular Newtonian Poiseuille flows and reviewed relevant works with Newtonian perturbation solutions. A linear equation of state is employed and the isothermal compressibility is taken as the perturbation parameter. Taliadorou et al. [21] and Joseph et al. [22] perturbed only the primary unknown fields, i.e. the pressure and the velocity vector, while Venerus [23,24] used a vorticity/streamfunction formulation. In the present work, the viscoelastic part of the stress tensor constitutes an additional primary field to be perturbed.

The rest of the paper is organized as follows. In Section 2, the governing equations, i.e., the equations of motion, the constitutive equation, and the equation of state are presented and then dedimensionalized to yield the basic dimensionless parameters, such as the compressibility parameter, the Weissenberg, and the Reynolds numbers. The perturbation procedure is described in Section 3 and the solution of the plane Poiseuille flow of an Oldroyd-B fluid is obtained up to second order in terms of the compressibility parameter. The correctness of all the expressions and the final perturbation solution derived here has been verified using "Mathematica" [25]. The results are analyzed in Section 4, where the effects of compressibility, the Weissenberg number, the Reynolds number and the aspect ratio on the velocity, the pressure and the stress fields are discussed. Finally, the main conclusions of this work are summarized in Section 5.

2. Governing equations

We consider the isothermal, steady, pressure-driven flow of a weakly compressible viscoelastic fluid between parallel plates and work in Cartesian coordinates centered at the midplane with the x-axis pointing in the main flow direction and the y-axis being vertical to the two plates. The gap between the plates is equal to $2H^*$ and their length and width are denoted by L^* and W^*, respectively. Note that throughout the paper a star "*" denotes that the corresponding quantity is dimensional.

For isothermal, steady flow with zero gravity, the dimensional forms of the continuity and momentum equations are:

$$\underline{\nabla}^* \cdot (\rho^* \underline{v}^*) = 0 \tag{1}$$

$$\rho^* \underline{v}^* \cdot \underline{\nabla}^* \underline{v}^* = \underline{\nabla}^* \cdot \underline{\underline{T}}^* \tag{2}$$

where ρ^* is the mass density of the fluid, $\underline{v}^*$ is the velocity vector, and $\underline{\underline{T}}^*$ is the total stress tensor, given by:

$$\underline{\underline{T}}^* = -p^* \underline{\underline{I}} + \eta_s^* \underline{\underline{\dot{\gamma}}}^* + \underline{\underline{\tau}}^* \tag{3}$$

where p^* is the total pressure, η_s^* is the constant zero shear-rate (Newtonian) viscosity of the pure solvent, $\underline{\underline{\dot{\gamma}}}^*$ is the augmented rate-of-strain tensor, and $\underline{\underline{\tau}}^*$ is the viscoelastic part of the extra-stress tensor (due to the polymer). For a compressible fluid with zero bulk viscosity, the augmented rate-of-strain tensor, $\underline{\underline{\dot{\gamma}}}^*$, is defined as:

$$\underline{\underline{\dot{\gamma}}}^* = \underline{\nabla}^* \underline{v}^* + (\underline{\nabla}^* \underline{v}^*)^T - \frac{2}{3}(\underline{\nabla}^* \cdot \underline{v}^*)\underline{\underline{I}} \tag{4}$$

where $\underline{\underline{I}}$ is the unit tensor and the superscript T denotes the transpose. The Oldroyd-B constitutive equation is:

$$\underline{\underline{\tau}}^* + \lambda^* \left[\frac{\partial \underline{\underline{\tau}}^*}{\partial t^*} + \underline{v}^* \cdot \underline{\nabla}^* \underline{\underline{\tau}}^* - \underline{\underline{\tau}}^* \cdot \underline{\nabla}^* \underline{v}^* - (\underline{\nabla}^* \underline{v}^*)^T \cdot \underline{\underline{\tau}}^* \right] = \eta_p^* \underline{\underline{\dot{\gamma}}}^* \tag{5}$$

where η_p^* and λ^* are the zero shear-rate viscosity and the single relaxation time of the polymer, respectively.

The fluid under consideration is assumed compressible with its mass density following a linear equation of state:

$$\rho^* = \rho_0^* [1 + \varepsilon^* (p^* - p_0^*)] \tag{6}$$

where ρ_0^* is the mass density at a reference pressure p_0^*, $\varepsilon^* = -(1/V_0^*)(\partial V^*/\partial P^*)_{P_0^*, T_0^*}$ is the isothermal compressibility coefficient, which is a assumed to be constant, V^* is the specific volume, and V_0^* is the specific volume at the reference pressure, p_0^*, and temperature, T_0^*.

Eqs. (1)–(6) are dedimensionalized by scaling the flow direction, x^*, by the length L^* of the channel, the transverse coordinate, y^*, by the channel half-width H^*, the axial velocity component, u_x^*, by a characteristic velocity U^*, the transverse velocity component, u_y^*, by U^*H^*/L^*, the mass density ρ^* by ρ_0^*, and the viscoelastic part of the extra-stress tensor, $\underline{\underline{\tau}}^*$, by $\eta_p^* U^*/L^*$. The characteristic velocity U^* is defined here as the mean velocity at the channel exit:

$$U^* \equiv \frac{\dot{M}^*}{\rho_0^* H^* W^*} \tag{7}$$

where $\dot{M}^*$ is the mass flow-rate at the outlet plane and W^* is the characteristic length in the neutral direction. Finally, the pressure difference $p^* - p_0^*$ is scaled by $3(\eta_s^* + \eta_p^*)L^*U^*/H^{*2}$ so that the dimensionless pressure gradient in the case of incompressible flow is equal to 1. Using these scales, the dimensionless forms of the continuity equation and the two components of the momentum equation become:

$$\frac{\partial(\rho u_x)}{\partial x} + \frac{\partial(\rho u_y)}{\partial y} = 0 \tag{8}$$

$$\alpha \,\mathrm{Re}\, \rho \left(u_x \frac{\partial u_x}{\partial x} + u_y \frac{\partial u_x}{\partial y} \right) = -3 \frac{\partial p}{\partial x} + \eta_s \left\{ \alpha^2 \frac{\partial^2 u_x}{\partial x^2} + \frac{\partial^2 u_x}{\partial y^2} + \frac{\alpha^2}{3} \left(\frac{\partial^2 u_x}{\partial x^2} + \frac{\partial^2 u_y}{\partial x \partial y} \right) \right\} + \eta_p \left\{ \alpha^2 \frac{\partial \tau_{xx}}{\partial x} + \alpha \frac{\partial \tau_{xy}}{\partial y} \right\} \tag{9}$$

$$\alpha^3 \,\mathrm{Re}\,\rho\left(u_x\frac{\partial u_y}{\partial x}+u_y\frac{\partial u_y}{\partial y}\right)=-3\frac{\partial p}{\partial y}+\eta_s\alpha^2\left\{\alpha^2\frac{\partial^2 u_y}{\partial x^2}+\frac{\partial^2 u_y}{\partial y^2}+\frac{1}{3}\left(\frac{\partial^2 u_x}{\partial x\partial y}+\frac{\partial^2 u_y}{\partial y^2}\right)\right\}+\eta_p\alpha^2\left\{\alpha\frac{\partial \tau_{xy}}{\partial x}+\frac{\partial \tau_{yy}}{\partial y}\right\} \tag{10}$$

where $\eta_s \equiv \eta_s^*/(\eta_s^*+\eta_p^*)$ and $\eta_p \equiv \eta_p^*/(\eta_s^*+\eta_p^*)$ are respectively the dimensionless viscosity ratios for the solvent and the polymer, $\alpha = H^*/L^*$ is the aspect ratio of the channel, and

$$\mathrm{Re} \equiv \frac{\rho_0^* U^* H^*}{\eta_s^*+\eta_p^*} \tag{11}$$

is the Reynolds number.

The dimensionless equations for the non-trivial components of the constitutive model are:

$$\tau_{xx}+\mathrm{We}\left(u_x\frac{\partial \tau_{xx}}{\partial x}+u_y\frac{\partial \tau_{xx}}{\partial y}-2\tau_{xx}\frac{\partial u_x}{\partial x}-\frac{2\tau_{xy}}{a}\frac{\partial u_x}{\partial y}\right)=\frac{4}{3}\frac{\partial u_x}{\partial x}-\frac{2}{3}\frac{\partial u_y}{\partial y} \tag{12}$$

$$\tau_{xy}+\mathrm{We}\left(u_x\frac{\partial \tau_{xy}}{\partial x}+u_y\frac{\partial \tau_{xy}}{\partial y}-\tau_{xy}\left(\frac{\partial u_x}{\partial x}+\frac{\partial u_y}{\partial y}\right)-\tau_{xx}a\frac{\partial u_y}{\partial x}-\frac{\tau_{yy}}{a}\frac{\partial u_x}{\partial y}\right)=\alpha\frac{\partial u_y}{\partial x}+\frac{1}{\alpha}\frac{\partial u_x}{\partial y} \tag{13}$$

$$\tau_{yy}+\mathrm{We}\left(u_x\frac{\partial \tau_{yy}}{\partial x}+u_y\frac{\partial \tau_{yy}}{\partial y}-2\tau_{yy}\frac{\partial u_y}{\partial y}-2a\tau_{xy}\frac{\partial u_y}{\partial x}\right)=\frac{4}{3}\frac{\partial u_y}{\partial y}-\frac{2}{3}\frac{\partial u_x}{\partial x} \tag{14}$$

$$\tau_{zz}+\mathrm{We}\left(u_x\frac{\partial \tau_{zz}}{\partial x}+u_y\frac{\partial \tau_{zz}}{\partial y}\right)=-\frac{2}{3}\left(\frac{\partial u_x}{\partial x}+\frac{\partial u_y}{\partial y}\right) \tag{15}$$

where

$$\mathrm{We} \equiv \frac{\lambda^* U^*}{L^*} \tag{16}$$

is the Weissenberg number.

Finally, the dimensionless form of the equation of state is:

$$\rho = 1+\varepsilon p \tag{17}$$

where

$$\varepsilon \equiv \frac{3(\eta_s^*+\eta_p^*)\varepsilon^* L^* U^*}{H^{*2}} \tag{18}$$

is the compressibility number.

Eqs. (8)–(10), (12)–(15) and (17) are defined in the domain $\{0 \le x \le 1,\ -1 \le y \le 1\}$. In addition to the viscosity ratios, η_s and η_p, four other dimensionless numbers appear; these are the aspect ratio and the Reynolds, Weissenberg and compressibility numbers: α, Re, We and ε. Note that the Mach number for this compressible flow takes the form

$$\mathrm{Ma} \equiv \sqrt{\frac{\varepsilon\alpha\,\mathrm{Re}}{\left(3\frac{c_p^*}{c_v^*}\right)}} \tag{19}$$

where c_p^*/c_v^* is the heat capacity ratio (or adiabatic index). In this work only subsonic flows are considered, so that $\mathrm{Ma} \ll 1$.

The governing partial differential equations are supplemented by suitable boundary conditions, i.e. no-slip and no-penetration at the wall ($y=1$), symmetry conditions at the midplane ($y=0$), a reference value for the pressure at $x=y=1$, and the condition that the total (dimensionless) mass flow-rate, $\dot{M}$, at the outlet plane ($x=1$) is equal to unity:

$$u_x(x,1)=u_y(x,1)=0, \quad 0 \le x \le 1 \tag{20}$$

$$\frac{\partial u_x}{\partial y}(x,0)=u_y(x,0)=0, \quad 0 \le x \le 1 \tag{21}$$

$$p(1,1)=0 \tag{22}$$

$$\dot{M}=\int_0^1 \rho u_x dy = 1 \quad \text{at } x=1 \tag{23}$$

Note that no boundary conditions are specified at the inlet plane ($x=0$), as discussed by Venerus [23], Poinsot and Lele [26], and Taliadorou et al. [21].

3. Perturbation solution

We employ a regular perturbation scheme in terms of the compressibility parameter, ε. Hence, the primary dependent variables are expanded as follows:

$$\left.\begin{aligned} p &= p_0 + \varepsilon p_1 + \varepsilon^2 p_2 + O(\varepsilon^3) \\ u_x &= u_{x0} + \varepsilon u_{x1} + \varepsilon^2 u_{x2} + O(\varepsilon^3) \\ u_y &= 0 + \varepsilon u_{y1} + \varepsilon^2 u_{y2} + O(\varepsilon^3) \\ \tau_{xx} &= \tau_{xx0} + \varepsilon \tau_{xx1} + \varepsilon^2 \tau_{xx2} + O(\varepsilon^3) \\ \tau_{xy} &= \tau_{xy0} + \varepsilon \tau_{xy1} + \varepsilon^2 \tau_{xy2} + O(\varepsilon^3) \\ \tau_{zz} &= \tau_{zz0} + \varepsilon \tau_{zz1} + \varepsilon^2 \tau_{zz2} + O(\varepsilon^3) \\ \rho &= 1 + \varepsilon \rho_1 + \varepsilon^2 \rho_2 + O(\varepsilon^3) \end{aligned}\right\} \tag{24}$$

The transverse velocity is assumed to be zero at zero order. The expansion of ρ is suggested explicitly by Eq. (17). The same choice of perturbation parameter was also made by Venerus [23] and, more recently, by Taliadorou et al. [21] and Joseph et al. [22] and Venerus and Bugajsky [24]. Schwartz [27] also employed the equivalent quantity $\mathrm{Ma}^2/\mathrm{Re}$.

Substituting the expansions of Eq. (24) into the governing equations and collecting together terms of the same order, a sequence of partial differential equations together with the accompanying boundary conditions is formed. The zero-, first-, and second-order problems are solved analytically below.

3.1. Zero-order problem

Zero-order equations are trivial and their solution is the following:

$$\left.\begin{aligned} p_0 &= 1 - x \\ u_{x0} &= \frac{3}{2}(1 - y^2) \\ u_{y0} &= 0 \\ \tau_{xx0} &= \frac{18\,\mathrm{We}}{\alpha^2} y^2 \\ \tau_{xy0} &= -\frac{3}{\alpha} y \\ \tau_{yy0} &= 0 \\ \tau_{zz0} &= 0 \\ \rho_0 &= 1 \end{aligned}\right\} \tag{25}$$

Eq. (25) is the standard solution for incompressible Poiseuille flow of an Oldroyd-B fluid. With the exception of τ_{xx0}, which depends on the Weissenberg number, the solution is the same as that for a Newtonian fluid [21,24].

3.2. First-order problem

The first-order terms of the equation of state is $\rho_1 = p_0$ which gives

$$\rho_1 = 1 - x \tag{26}$$

The first-order terms of the continuity equation then becomes:

$$\frac{\partial}{\partial x}(\rho_1 u_{x0} + u_{x1}) + \frac{\partial}{\partial y}(u_{y1}) = 0 \tag{27}$$

Assuming that $u_{y1} = 0$ (an assumption also made in [21–24] for the Newtonian flow), so that we can derive a separable solution, and integrating the above equation with respect to x, we get the following expression for u_{x1}:

$$u_{x1}(x, y) = x u_{x0}(y) + f(y) \tag{28}$$

where $f = f(y)$ is a function to be determined. From Eq. (28) and the boundary conditions for u_x in Eqs. (20), (21) and (23), it is deduced that f satisfies the following three conditions:

$$f(1) = \frac{df}{dy}(0) = 0 \quad \text{and} \quad \int_0^1 f(y)dy = -1 \tag{29}$$

The y-momentum at $O(\varepsilon^1)$ takes the form:

$$\frac{\partial p_1}{\partial y} = \frac{2}{3} a^2 \eta_p y - \frac{1}{3} \eta_s a^2 y + \frac{1}{3} a^3 \eta_p \frac{\partial \tau_{xy1}}{\partial x} \tag{30}$$

which is integrated with respect to y to give the following expression for p_1:

$$p_1 = \frac{1}{3}a^2y^2\left(\eta_p - \frac{1}{2}\eta_s\right) + \frac{1}{3}a^3\eta_p\int\frac{\partial\tau_{xy1}}{\partial x}dy + g(x) \tag{31}$$

where $g = g(x)$ in another unknown function to be determined. The extra stress component τ_{xy1} can be found from the first-order xy-component of the constitutive model. However, in this equation τ_{yy1} is required. Following the procedure described in Appendix A, and solving the corresponding first order equation for τ_{zz1} as well, we find that

$$\tau_{yy1} = \tau_{zz1} = y^2 - 1 \tag{32}$$

Similarly, we get

$$\tau_{xy1} = \frac{1}{\alpha}\left[y(-3x + 2\,\mathrm{We}\,u_{x0}) + \frac{df}{dy}\right] \tag{33}$$

Substituting the above expression into Eq. (31) and simplifying we get:

$$p_1 = -\frac{1}{6}a^2y^2 + g(x) \tag{34}$$

From Eqs. (34) and (22), we obtain the following condition for g:

$$g(1) = \frac{\alpha^2}{6} \tag{35}$$

Next, we calculate τ_{xx1} from the corresponding component of the constitutive model, following once again the procedure described in Appendix A:

$$\tau_{xx1} = \frac{12\,\mathrm{We}}{\alpha^2}\left[3y^2(x - u_{x0}\mathrm{We}) + y\left(2y\,\mathrm{We}\,u_{x0} - \frac{df}{dy}\right)\right] + \frac{4}{3}u_{x0} \tag{36}$$

Substituting Eq. (36) into the first-order terms of the x-momentum equation and separating variables lead to

$$\frac{9a}{4}\mathrm{Re}(y^2-1)^2 - 3\eta_p\,\mathrm{We}(1+9y^2) - \frac{d^2f}{dy^2} = -3\left(\frac{dg}{dx} + x\right) \tag{37}$$

The above equation is valid when each side is equal to a constant, c_1; thus, we obtain the following ODEs for f and g:

$$\frac{9a}{4}\mathrm{Re}(y^2-1)^2 - 3\eta_p\,\mathrm{We}(1+9y^2) - \frac{d^2f}{dy^2} = c_1 \tag{38}$$

and

$$-3\left(\frac{dg}{dx} + x\right) = c_1 \tag{39}$$

Integrating Eq. (38) and applying the conditions for f (see Eq. (29)), we calculate the two integration constants and then c_1, getting:

$$c_1 = \frac{6}{35}(9\alpha\,\mathrm{Re} - 49\eta_p\,\mathrm{We}) - 3 \tag{40}$$

and

$$f(y) = (1-y^2)\left[-\frac{3}{2} + \frac{3a}{280}\mathrm{Re}(-5 + 28y^2 - 7y^4) + \frac{9}{20}\eta_p\,\mathrm{We}(-1+5y^2)\right] \tag{41}$$

Integrating now Eq. (39) and using Eqs. (34) and (40), we get:

$$g(x) = \frac{\alpha^2}{6} - \frac{1}{2}(1-x)^2 + \frac{2}{35}(1-x)[9\alpha\,\mathrm{Re} - 49\eta_p\,\mathrm{We}] \tag{42}$$

Substituting f in Eqs. (28), (33) and (36), and g into Eq. (34) completes the first-order solution.

3.3. Second-order problem

From the second-order terms of the equation of state, we get

$$\rho_2 = p_1 = -\frac{1}{6}a^2y^2 + \frac{\alpha^2}{6} - \frac{1}{2}(1-x)^2 + \frac{2}{35}(1-x)(9\alpha\,\mathrm{Re} - 49\eta_p\,\mathrm{We}) \tag{43}$$

Now, the second-order component of the continuity equation can be written as follows:

$$\frac{\partial u_{x2}}{\partial x} + \frac{\partial u_{y2}}{\partial y} + \frac{\partial}{\partial x}(p_0u_{x1}) + \frac{\partial p_1}{\partial x}u_{x0} = 0 \tag{44}$$

Assuming that $u_{y2} = u_{y2}(y)$ and integrating with respect to x give:

$$u_{x2} = p_0\left(\frac{du_{y2}}{dy} - u_{x1}\right) - p_1u_{x0} + F(y)$$

where F is a function to be determined. Substituting p_0, u_{x1}, p_1 in the above equation we get:

$$u_{x2} = \frac{3}{2}x^2 u_{x0} - x\left[\left(1-\frac{c_1}{3}\right)u_{x0} - f + \frac{du_{y2}}{dy}\right] + \frac{du_{y2}}{dy} - f + F - u_{x0}\left[\frac{a^2}{6}(1-y^2) + \frac{1}{2} + \frac{c_1}{3}\right] \tag{45}$$

Integrating the second-order terms of the y-momentum equation,

$$0 = -3\frac{\partial p_2}{\partial y} + \eta_s\left(\frac{4\alpha^2}{3}\frac{d^2u_{y2}}{dy^2} + \frac{\alpha^2}{3}\frac{\partial^2 u_{x2}}{\partial x \partial y}\right) + \eta_p\alpha^2\left(\alpha\frac{\partial \tau_{xy2}}{\partial x} + \frac{\partial \tau_{yy2}}{\partial y}\right) \tag{46}$$

with respect to y and rearranging some terms, we obtain the following expression for p_2:

$$p_2 = \frac{\eta_s}{9}\alpha^2\left(4\frac{du_{y2}}{dy} + \frac{\partial u_{x2}}{\partial x}\right) + \frac{\eta_p}{3}\alpha^2\left(\tau_{yy2} + \alpha\int\frac{\partial \tau_{xy2}}{\partial x}dy\right) + G(x) \tag{47}$$

where G is another function to be determined. The second-order stress components τ_{yy2} and τ_{xy2} can be found by solving the corresponding components of the constitutive equation:

$$\tau_{yy2} + \mathrm{We}\,u_{x0}\frac{\partial \tau_{yy2}}{\partial x} = \frac{4}{3}\frac{du_{y2}}{dy} - \frac{2}{3}\frac{\partial u_{x2}}{\partial x} \tag{48}$$

$$\tau_{xy2} + \mathrm{We}\,u_{x0}\frac{\partial \tau_{xy2}}{\partial x} = \frac{1}{\alpha}\frac{\partial u_{x2}}{\partial y} + \mathrm{We}\left[\frac{3u_{y2}}{\alpha} + \tau_{xy1}u_{x0} - \tau_{xy0}u_{x1} + \tau_{xy0}\left(\frac{du_{y2}}{dy} + \frac{\partial u_{x2}}{\partial x}\right) + \frac{1}{a}\left(\tau_{yy1}\frac{\partial u_{x1}}{\partial y} + \tau_{yy2}\frac{du_{x0}}{dy}\right)\right] \tag{49}$$

where the relations $u_{x0} = \partial u_{x1}/\partial x$ and $\tau_{xy0} = \partial \tau_{xy1}/\partial x$ have been used. Taking into account that $\partial^2 u_{x1}/\partial x^2 = 0$, using Eq. (45), and following the procedure described in Appendix A, we can solve Eq. (48) for τ_{yy2} :

$$\tau_{yy2} = -2u_{x0}\left(x - u_{x0}\,\mathrm{We} - \frac{1}{3} + \frac{c_1}{9}\right) + 2\frac{du_{y2}}{dy} - \frac{2f}{3} \tag{50}$$

The shear stress component τ_{xy2} can now be found from Eq. (49):

$$\tau_{xy2} = -\frac{9y}{a}\left(\mathrm{We}^2u_{x0}^2 - \mathrm{We}\,u_{x0}x + \frac{1}{2}x^2\right) + a_1(y)(x - \mathrm{We}\,u_{x0}) + a_0(y) \tag{51}$$

where

$$a_1(y) = \frac{1}{\alpha}\left[-yu_{x0}\,\mathrm{We} + \frac{\partial^2 u_{x2}}{\partial x \partial y}(0,y)\right] \tag{52}$$

and

$$a_0(y) = \frac{1}{\alpha}\frac{\partial u_{x2}}{\partial y}(0,y) + \mathrm{We}\left\{\frac{3(u_{y2}+yf)}{\alpha} + u_{x0}\tau_{xy1}(0,y) + \tau_{xy0}\left[\frac{du_{y2}}{dy} + \frac{\partial u_{x2}}{\partial x}(0,y)\right] + \frac{1}{a}\left[\tau_{yy1}\frac{df}{dy} + \frac{du_{x0}}{dy}\tau_{yy2}(0,y)\right]\right\} \tag{53}$$

The second-order component of the x-momentum equation is:

$$\alpha\,\mathrm{Re}\left[u_{x0}\left(\rho_1\frac{\partial u_{x1}}{\partial x} + u_{x1} + \frac{\partial u_{x2}}{\partial x}\right) + u_{y2}\frac{du_{x0}}{dy}\right] = -3\frac{\partial p_2}{\partial x} + \eta_s\left(4\alpha^2u_{x0} + \frac{\partial^2 u_{x2}}{\partial y^2}\right) + \alpha\eta_p\left(\alpha\frac{\partial \tau_{xx2}}{\partial x} + \frac{\partial \tau_{xy2}}{\partial y}\right) \tag{54}$$

From the second-order xx-component of the constitutive equation,

$$\tau_{xx2} + \mathrm{We}\,u_{x0}\frac{\partial \tau_{xx2}}{\partial x} = \frac{4}{3}\frac{\partial u_{x2}}{\partial x} - \frac{2}{3}\frac{du_{y2}}{dy} + \mathrm{We}\left[-u_{x1}\frac{\partial \tau_{xx1}}{\partial x} - u_{y2}\frac{d\tau_{xx0}}{dy} + 2\frac{\partial u_{x2}}{\partial x}\tau_{xx0} + 2u_{x0}\tau_{xx1} + \frac{2}{a}\left(\frac{\partial u_{x2}}{\partial y}\tau_{xy0} + \frac{\partial u_{x1}}{\partial y}\tau_{xy1} + \frac{du_{x0}}{dy}\tau_{xy2}\right)\right] \tag{55}$$

and following the procedure described in Appendix A, we solve for τ_{xx2} :

$$\tau_{xx2} = \frac{144\,\mathrm{We}}{\alpha^2}y^2\left(\mathrm{We}^2u_{x0}^2 - \mathrm{We}\,u_{x0}x + \frac{1}{2}x^2\right) + b_1(y)(x - \mathrm{We}\,u_{x0}) + b_0(y) \tag{56}$$

where

$$b_1(y) = 4u_{x0}\left[1 + \left(\frac{3\,\mathrm{We}\,y}{\alpha}\right)^2\right] + 2\,\mathrm{We}\left\{3u_{x0}\tau_{xx0} + \frac{\tau_{xy0}}{a}\left[-\frac{d^2u_{y2}}{dy^2} + 3y\left(1-\frac{c_1}{3}\right) + 2\frac{df}{dy}\right] - \frac{3y}{a}\left[\tau_{xy1}(0,y) + \frac{9y}{\alpha}\mathrm{We}\,u_{x0} + a_1(y)\right]\right\} \tag{57}$$

and

$$b_0(y) = -\frac{36\,\mathrm{We}^2y(yf+u_{y2})}{\alpha^2} + \left(\frac{4}{3} + 2\,\mathrm{We}\,\tau_{xx0}\right)\frac{\partial u_{x2}}{\partial x}(0,y) - \frac{2}{3}\frac{du_{y2}}{dy} + 2\,\mathrm{We}\left[u_{x0}\tau_{xx1}(0,y) + \frac{1}{a}\left(\frac{\partial u_{x2}}{\partial y}(0,y)\tau_{xy0} + \frac{df}{dy}\tau_{xy1}(0,y) + \frac{du_0}{dy}\tau_{xy2}(0,y)\right)\right] \tag{58}$$

In Eq. (58), $\partial u_{x2}/\partial x(0,y)$ and $\partial u_{x2}/\partial y(0,y)$ are found from Eq. (45) while the terms $\tau_{xx1}(0,y)$, $\tau_{xy1}(0,y)$ and $\tau_{xy2}(0,y)$ are found from Eqs. (35), (32) and (51), respectively. Substituting the expressions for ρ_1, u_{x1}, τ_{xx2}, τ_{xy2} and p_2 into Eq. (54) and simplifying the result leads to an equation of the following form:

$$xs_1(y, u_{y2}(y)) + s_2(y, u_{y2}(y), F(y)) + s_3(x, G(x)) = 0 \tag{59}$$

where s_1, s_2 and s_3 are known functions:

$$s_1(y, u_{y2}(y)) = 9\alpha\,\mathrm{Re}\left[-\frac{59}{70} + y^2\left(1 - \frac{y^2}{2}\right)\right] + \mathrm{We}\,\eta_p\left(\frac{129}{5} + 81y^2\right) - \frac{d^3u_{y2}}{dy^3} \tag{60}$$

$$s_3(x, G(x)) = -\frac{9}{2}x^2 + 9x - 3\frac{dG}{dx} \tag{61}$$

while s_2 is too long to be given here; however, it is available upon request. Eq. (59) is valid for any x and y, only if $s_1 = \gamma$, $s_2 = c_2$, and $x\gamma + c_2 + s_3 = 0$, where γ and c_2 are constants to be determined. These three equations, together with the appropriate auxiliary conditions, determine the unknowns functions $u_{y2} = u_{y2}(y)$, $F = F(y)$ and $G = G(x)$. Indeed, the first equation, $s_1 = \gamma$, is solved with the required auxiliary conditions, which also allow for the evaluation of γ.

First, Eq. (20) at second order gives $u_{x2}(x, 1) = 0$, which in conjunction with Eq. (45), results in:

$$(1-x)\left[\frac{du_{y2}}{dy}(1) - xu_{x0}(1) - f(1)\right] - p_1(1,y)u_{x0}(1) + F(1) = 0. \tag{62}$$

Since $f(1) = u_{x0}(1) = 0$ and the latter equation must hold for any x, it follows that $(du_{y2}/dy)(1) = F(1) = 0$. Eqs. (20) and (21) give $u_{y2}(0) = u_{y2}(1) = 0$. Moreover, by differentiating Eq. (45) with respect to y and using boundary condition (21) give

$$\frac{\partial u_{x2}}{\partial y}(x,0) = (1-x)\left(\frac{d^2u_{y2}}{dy^2} - x\frac{du_{x0}}{dy} - \frac{df}{dy}\right)(0) - \frac{\partial p_1}{\partial y}(x,0)u_{x0}(0) - p_1(x,0)\frac{du_{x0}}{dy}(0) + F'(0) = 0 \tag{63}$$

Since $(du_{x0}/dy)(0) = (df/dy)(0) = 0$, and $(\partial p_1/\partial y)(x,0) = 0$ (see Eq. (34)), we get

$$(1-x)\frac{d^2u_{y2}}{dy^2}(0) + F'(0) = 0$$

and therefore $(d^2u_{y2}/dy^2)(0) = F'(0) = 0$. Summarizing, the boundary conditions for u_{y2} are:

$$u_{y2}(0) = u_{y2}(1) = \frac{du_{y2}}{dy}(1) = \frac{d^2u_{y2}}{dy^2}(0) = 0 \tag{64}$$

Then, the solution of $s_1 = \gamma$ is:

$$u_{y2} = \frac{3}{140}y(1-y^2)^2[\alpha\,\mathrm{Re}(5-y^2) + 63\eta_p\,\mathrm{We}] \tag{65}$$

and

$$\gamma = -\frac{216}{35}\alpha\,\mathrm{Re} + 42\eta_p\,\mathrm{We} \tag{66}$$

It is clear that inertia and viscoelasticity give rise to non-zero transverse velocity, u_{y2}.

Now, from $x\gamma + c_2 + s_3 = 0$ and Eq. (61) we have:

$$-\frac{9}{2}x^2 + (9+\gamma)x - 3\frac{dG}{dx} = -c_2 \tag{67}$$

which can be integrated to yield:

$$G(x) = -\frac{1}{2}x^3 + \frac{1}{6}(9+\gamma)x^2 + \frac{c_2}{3}x + c_3 \tag{68}$$

where c_3 is another constant to be determined. Last, by substituting u_{y2} in $s_2(y, u_{y2}, F) = c_2$ we get a second-order ordinary differential equation for F which is integrated twice with respect to y along with the required auxiliary conditions for F:

$$\int_0^1 F(y)dy = 0, \quad F(1) = 0, \quad \frac{dF}{dy}(0) = 0 \tag{69}$$

Eq. (69) results from the total mass flow-rate, Eq. (23), at second order, which is

$$\dot{M}_2 = \frac{1}{2}\int_{-1}^{+1}(\rho_2 u_{x0} + \rho_1 u_{x1} + u_{x2})dy = 0 \quad \text{at } x = 1$$

and from $\rho_2(1,y) = p_1(1,y)$, $\rho_1(1) = p_0(1) = 0$ and $u_{x2}(1,y) = -p_1(1,y)u_{x0}(y) + F(y)$.

Solving $s_2 = c_2$ and applying the three auxiliary conditions given in Eq. (69), c_2 and F can be determined:

$$c_2 = -\frac{9}{2} + \alpha^2\left(\frac{17 - 9\eta_s}{2} - \frac{9132\,\mathrm{Re}^2}{13,475}\right) - 42\eta_p We + \frac{12}{175}\eta_p\,\mathrm{We}^2(-829 + 589\eta_s) + \frac{\alpha\,\mathrm{Re}}{35}\left(216 + \frac{1478}{5}\eta_p\,\mathrm{We}\right) \tag{70}$$

$$F(y) = (1-y^2)\left\{\frac{\alpha^2}{8}(1-5y^2) + \frac{3\alpha^2\,\mathrm{Re}^2}{431200}(-2193+9163y^2+6853y^4-5159y^6+616y^8)\right.$$
$$\left. -\frac{3\eta_p\,\mathrm{We}^2}{1400}[-201\eta_s+561+(420\eta_s-2520)y^2+(1365\eta_s-665)y^4] - \frac{\eta_p a\,\mathrm{We}\,\mathrm{Re}}{11,200}(1303-1413y^2-13,563y^4+2985y^6)\right\} \tag{71}$$

The constant c_3 is determined with the aid of the suitable boundary condition for the pressure, which results from Eq. (22) at $O(\varepsilon^2)$:

$$p_2(1,1) = 0 \tag{72}$$

Indeed, using Eq. (47) and $(du_{y2}/dy)(1) = (\partial u_{x2}/\partial x)(1,1) = \tau_{yy2}(1,1) = 0$, we get:

$$0 = p_2(1,1) = \frac{\eta_p}{3}\alpha^3\left(\int \frac{\partial \tau_{xy2}}{\partial x}dy\right)(1,1) + G(1) \tag{73}$$

The integral in Eq. (73) is calculated using Eq. (51). The solution for c_3 is:

$$c_3 = \frac{1}{2} + \frac{57}{280}a^3\eta_p\,\mathrm{Re} - \frac{2}{525}a\,\mathrm{Re}(270+739\eta_p\,\mathrm{We}) + -\frac{\eta_p\,\mathrm{We}}{175}\left\{-1225+4\,\mathrm{We}(-829+589\eta_s)\right.$$
$$\left. + a^2\left[-\frac{17}{6} + \frac{3044}{13,475}\mathrm{Re}^2 - \mathrm{We}(3+2\eta_s^2) + \eta_s\left(\frac{3}{2}+5\,\mathrm{We}\right)\right]\right\} \tag{74}$$

Substituting γ, c_2, c_3 into Eq. (68) and simplifying the result we find the solution for G:

$$G(x) = \frac{1}{2}(1-x)^3 - \frac{17-9\eta_s}{6}\alpha^2(1-x) - \frac{36}{35}\alpha\,\mathrm{Re}(1-x)^2 + \frac{3044}{13,475}\alpha^2\,\mathrm{Re}^2(1-x)$$
$$+ \frac{57}{280}\eta_p a^3\,\mathrm{Re} + \eta_p\,\mathrm{We}\left\{a^2(2\eta_s-3) + 7(1-x)^2 + \frac{2}{525}(1-x)[6\,\mathrm{We}(829-589\eta_s) - 739a\,\mathrm{Re}]\right\} \tag{75}$$

The second-order solution is completed by solving the zz-component of the constitutive equation,

$$\tau_{zz2} + \mathrm{We}\,u_{x0}\frac{\partial \tau_{zz2}}{\partial x} = -\frac{2}{3}\left(\frac{\partial u_{x2}}{\partial x} + \frac{du_{y2}}{dy}\right) \tag{76}$$

which gives:

$$\tau_{zz2} = -3(1-y^2)\left(x - \mathrm{We}\,u_{x0} - \frac{1}{3} + \frac{c_1}{9}\right) - \frac{2f}{3} \tag{77}$$

3.4. The perturbation solution up to second order

By combining the zero-, first- and second-order solutions derived above and rearranging some terms, we get the following expressions for the pressure, the velocity, and the extra stress components.

3.4.1. Pressure

$$p = 1 - x + \varepsilon\left[\frac{\alpha^2}{6}(1-y^2) - \frac{1}{2}(1-x)^2 + \frac{2}{35}(1-x)(9\alpha\,\mathrm{Re} - 49\eta_p\,\mathrm{We})\right] + \varepsilon^2\left\{\frac{1}{2}(1-x)^3 + \frac{\alpha^2}{6}(1-x)(-11+3y^2)\right.$$
$$+ \frac{3044\alpha^2\,\mathrm{Re}^2}{13,475}(1-x) - \frac{36}{35}\alpha\,\mathrm{Re}(1-x)^2 + \frac{a^3\,\mathrm{Re}}{840}(1-y^2)(97-140y^2+35y^4)$$
$$\left. + \mathrm{We}\,\eta_p\left[7(1-x)^2 - \frac{\alpha^2}{30}(1-y^2)(-13+75y^2) - \frac{1478}{525}\alpha\,\mathrm{Re}(1-x) - \frac{4\,\mathrm{We}}{175}(1-x)(-829+589\eta_s)\right]\right\} \tag{78}$$

3.4.2. Velocity components

$$u_x = \frac{3}{2}(1-y^2)\left\{1 + \varepsilon\left[-(1-x) + \frac{\alpha\,\mathrm{Re}}{140}(-5+28y^2-7y^4) + \frac{3\eta_p\,\mathrm{We}}{10}(-1+5y^2)\right] + \varepsilon^2\hat{u}_{x2}\right\} \tag{79}$$

where

$$\hat{u}_{x2} = \frac{3}{2}(1-x)^2 - \frac{\alpha^2}{12}(1+3y^2) + \frac{3\alpha\,\mathrm{Re}}{140}(1-x)(-19-28y^2+7y^4) - \frac{\alpha\eta_p\,\mathrm{Re}\,\mathrm{We}}{16,800}(1303-1413y^2-13,563y^4+2985y^6)$$
$$+ 2\eta_p\,\mathrm{We}(1-x)(2-3y^2) - \frac{\eta_p\,\mathrm{We}^2}{700}[561-201\eta_s+(420\eta_s-2520)y^2+(1365\eta_s-665)y^4]$$
$$- \frac{a^2\,\mathrm{Re}^2}{215,600}(2193-9163y^2-6853y^4+5159y^6-616y^8) \tag{80}$$

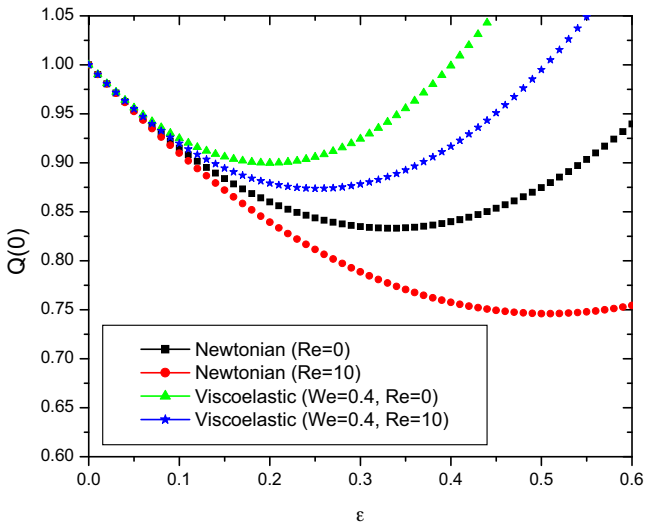

Fig. 1. The volumetric flow rate at the inlet of the channel, $Q(0)$, as a function of the compressibility parameter, ε, for $\alpha = 0.1$, $\eta_s = 1/9$, $\eta_p = 8/9$.

$$u_y = \frac{3\varepsilon^2}{140} y(1-y^2)^2[\alpha\,\mathrm{Re}(5-y^2) + 63\eta_p\,\mathrm{We}] \tag{81}$$

3.4.3. Extra stress components

$$\tau_{xx} = \frac{18\,\mathrm{We}}{\alpha^2}y^2 + \varepsilon\left\{2(1-y^2) + \frac{18\,\mathrm{We}^2 y^2}{a^2}\left[\frac{18\eta_s - 23}{5} + (7-6\eta_s)y^2\right]\right.$$
$$\left. + \mathrm{We}\,y^2\left[\frac{36}{\alpha}(x-1) + \mathrm{Re}\frac{y^2}{a}\left(-\frac{297}{35} + 18y^2 - \frac{27}{5}y^4\right)\right]\right\} + \varepsilon^2\tau_{xx2} \tag{82}$$

where

$$\tau_{xx2} = \left[\frac{26}{35}\alpha\,\mathrm{Re} - 6(1-x) + \frac{\mathrm{We}}{10}(89\eta_s - 119)\right] + \left[-\frac{96,597}{107,800}\mathrm{Re}^2\,We + \frac{9(24,421 - 15,997\eta_s + 1026\eta_s^2)\mathrm{We}^3}{350a^2}\right.$$
$$\left. + \mathrm{Re}\left(\frac{6a}{7} - \frac{3(-4868 + 1103\eta_s)\mathrm{We}^2}{350a} - \frac{108\,\mathrm{We}(x-1)}{7a}\right)\right]y^2 + \left[\frac{3}{2}(-25 + 11\eta_s)\mathrm{We} - \frac{243\,\mathrm{Re}^2\,\mathrm{We}}{70}\right.$$
$$\left. - \frac{81(109 - 97\eta_s + 18\eta_s^2)\mathrm{We}^3}{5a^2} + \mathrm{Re}\left(-2a + \frac{9(-370 + 171\eta_s)\mathrm{We}^2}{14a} + \frac{72\,\mathrm{We}(x-1)}{a}\right)\right]y^4$$

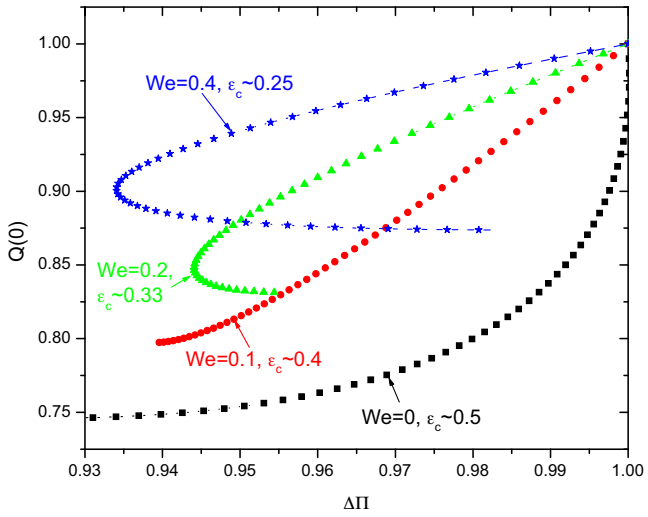

Fig. 2. The volumetric flow rate at the inlet of the channel, $Q(0)$, versus the pressure drop, $\Delta\Pi$, for a Newtonian and three viscoelastic fluids. Parameter values are $\alpha = 0.01$, $\mathrm{Re} = 100$, $\eta_s = 1/9$, $\eta_p = 8/9$. For each case, the critical compressibility number, ε_c, is also reported.

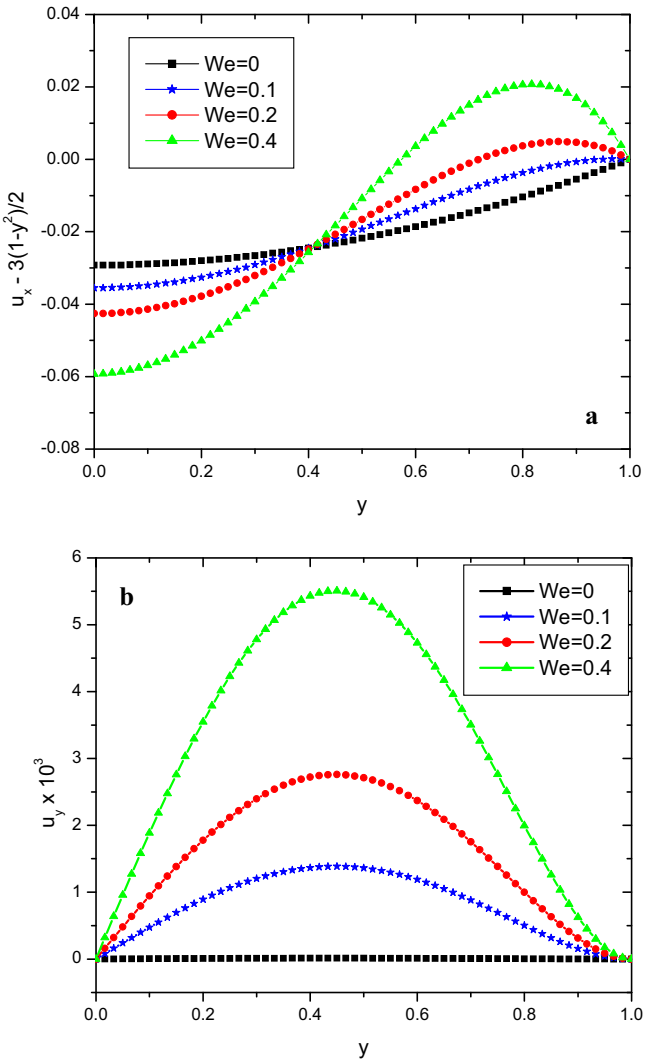

Fig. 3. Effect of the Weissenberg number on the velocity components in compressible Poiseuille flow: (a) deviation of u_x from the incompressible (parabolic) profile and (b) transverse velocity, u_y; $\varepsilon = 0.2$, $x = 0.9$, $\alpha = 0.01$, $\eta_s = 1/9$, $\mathrm{Re} = 1$.

$$+\left[\frac{1179\,\mathrm{Re}^2\,\mathrm{We}}{100}+\frac{27(481-529\eta_s+138\eta_s^2)\mathrm{We}^3}{10a^2}+\mathrm{Re}\left(\frac{2a}{5}-\frac{9(-328+189\eta_s)\mathrm{We}^2}{10a}-\frac{108\,\mathrm{We}(x-1)}{5a}\right)\right]y^6$$
$$+\left[-\frac{459\,\mathrm{Re}^2\,\mathrm{We}}{70}+\frac{9\,\mathrm{Re}\,\mathrm{We}}{70a}(325\eta_s-554)\right]y^8+\frac{1287}{1400}\,\mathrm{Re}^2\,\mathrm{We}\,y^{10} \tag{83}$$

$$\tau_{xy}=-\frac{3}{\alpha}y+\varepsilon y\left[\frac{3(1-x)}{\alpha}+9\,\mathrm{We}(1-\eta_s)\left(\frac{3}{5}-y^2\right)+3\,\mathrm{We}(1-y^2)+\frac{3\,\mathrm{Re}}{140}(33-70y^2+21y^4)\right]+\varepsilon^2 y\hat{\tau}_{xy2} \tag{84}$$

where:

$$\hat{\tau}_{xy2}=\frac{\alpha}{2}+\frac{8517}{53,900}a\,\mathrm{Re}^2+\frac{3}{700a}(-13,264+6343\eta_s+621\eta_s^2)-\frac{\mathrm{Re}}{1400}[1721+679\eta_s+810(1-x)]-\frac{6}{a}\mathrm{We}(7-5\eta_s)(1-x)$$
$$-\frac{9}{2\alpha}(1-x+x^2)+\left\{\frac{3a}{2}-\frac{9}{140}a\,\mathrm{Re}^2+\frac{3}{10a}(572-419\eta_s+27\eta_s^2)\mathrm{We}^2+\frac{3}{280}\mathrm{Re}[(1481-405\eta_s)\mathrm{We}-420(1-x)]\right.$$
$$\left.+\frac{12}{a}\mathrm{We}(4-3\eta_s)(1-x)\right\}y^2-\left\{\frac{351}{700}a\,\mathrm{Re}^2+\frac{9}{20a}(280-259\eta_s+39\eta_s^2)+\frac{9Re}{200}[(477-179\eta_s)\mathrm{We}+30(1-x)]\right\}y^4$$
$$+\frac{3}{280}(459-199\eta_s-30a\,\mathrm{Re}^2)y^6-\frac{3}{70}a\,\mathrm{Re}^2\,y^8 \tag{85}$$

$$\tau_{yy}=-\varepsilon(1-y^2)\left\{1-\varepsilon\left[3(1-x)+\frac{\mathrm{We}}{10}(103-58\eta_s+15(-13+10\eta_s)y^2)-\frac{\alpha\,\mathrm{Re}}{140}(37+196y^2-49y^4)\right]\right\} \tag{86}$$

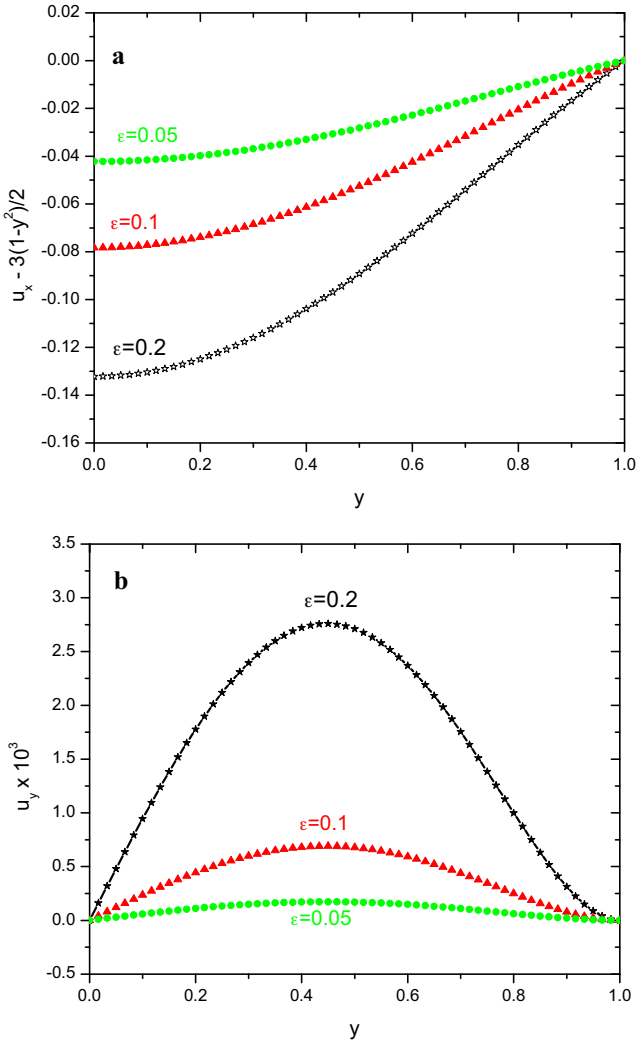

Fig. 4. Effect of the compressibility parameter, ε, on the velocity components: (a) deviation of u_x from the incompressible (parabolic) profile and (b) transverse velocity, u_y; We = 0.2, x = 0.9, α = 0.01, η_s = 1/9, Re = 1.

$$\tau_{zz} = -\varepsilon(1-y^2)\left\{1-\varepsilon\left[3(1-x)+\frac{\mathrm{We}}{10}(-76+31\eta_s-15(-4+\eta_s)y^2)-\frac{\alpha\,\mathrm{Re}}{140}(67+28y^2-7y^4)\right]\right\} \tag{87}$$

It is readily verified that for We = 0 the above expressions are reduced to the Newtonian solution obtained by Taliadorou et al. [21] and subsequently by Venerus and Bugajsky in [24].

4. Results and discussion

The basic features of the perturbation solution derived in Section 3 are the following:

(a) At zero order, the dimensionless pressure is independent of all dimensionless numbers in the flow problem. At first order both Re and We contribute separately, while at second order they contribute to the solution not only separately but also in combination. The y-dependence of pressure becomes stronger as α increases, i.e. as the length of the channel is reduced. At first order, the pressure gradient in the wall normal direction, $\partial p_1/\partial y$, is always positive below the midplane (respectively, negative above the midplane) and is due to viscous forces only, while $\partial p_1/\partial x$ depends on viscous forces, inertia and fluid viscoelasticity.
(b) The streamwise velocity component, u_x, deviates from the parabolic, incompressible, solution at first order in ε, due to fluid inertia and viscoelasticity. The contribution of the latter is negative for $|y| < 1/\sqrt{5}$ and positive otherwise, i.e. the streamwise velocity decreases close to the centerline and increases close to the walls. At second order, the effects of fluid inertia and viscoelasticity are combined.
(c) The transverse velocity component, u_y, is by assumption second order in ε. This is always positive above the midplane and varies linearly with the aspect ratio, the Reynolds, and the Weissenberg number.
(d) The density follows the same trends as the pressure (see Eq. (17)). At the exit of the channel (x = 1), we get:

$$\rho(x=1) = 1+\frac{\alpha^2\varepsilon^2}{6}(1-y^2)\left\{1+\varepsilon\,\mathrm{We}\,\eta_p\left(25y^2-\frac{13}{5}\right)+\varepsilon\alpha\,\mathrm{Re}\left(\frac{1}{4}y^4-y^2+\frac{97}{140}\right)\right\}+O(\varepsilon^4) \tag{88}$$

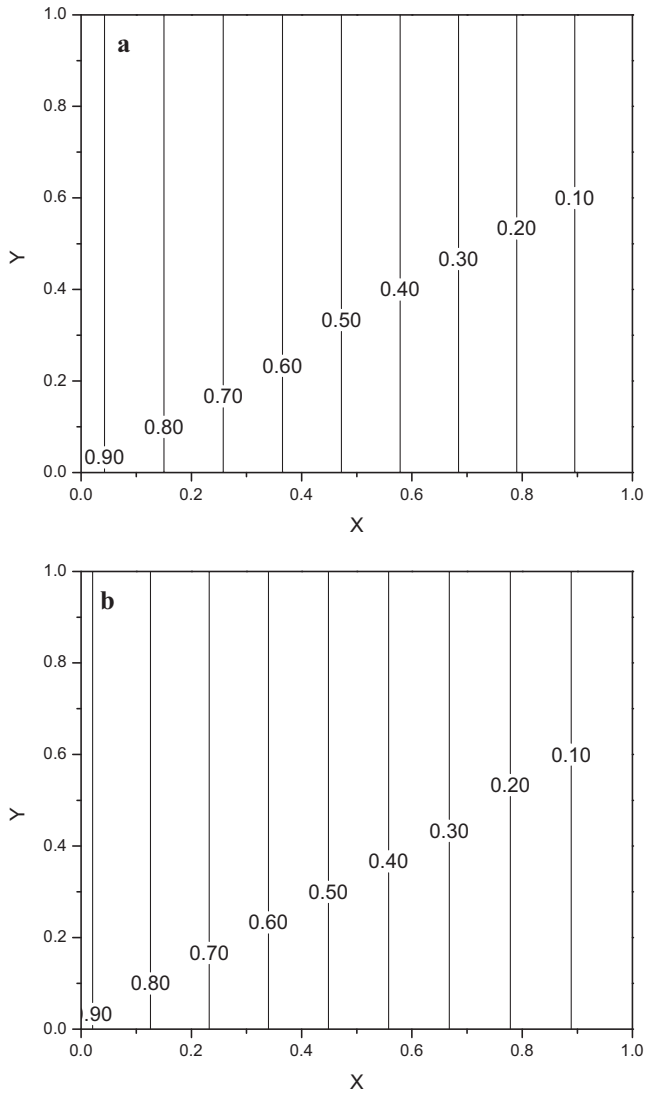

Fig. 5. Pressure field contours for We = 0.4, $\alpha = 0.01$, $\eta_s = 1/9$, and Re = 1: (a) $\varepsilon = 0.05$ and (b) $\varepsilon = 0.2$.

It is clear that at first order there is no effect of fluid inertia and viscoelasticity on the density. Since only very small variations of the density are acceptable at the exit of the channel (the fluid is decompressed and the mass density reaches its lowest values at $x = y = 1$), it is deduced that there must be $\varepsilon^2\alpha^2/6 \ll 1$.

(e) All non-zero components of the extra-stress tensor depend linearly on the Reynolds and Weissenberg numbers. In addition, there is a combined fluid inertia – viscoelasticity effect in the expression for τ_{xx}. For long channels and moderate Re and We, the major contribution to τ_{xx} at first order is that of We/α. For τ_{xy}, however, the viscous contribution is the most important at all orders, since this component is inversely proportional to the aspect ratio, α, for which $\alpha \ll 1$, dominating the viscoelastic and inertia contributions. Therefore, the differences of the τ_{xy} between the Newtonian and the viscoelastic cases are negligible. The expressions for τ_{yy} and τ_{zz} are similar; their magnitudes are much smaller than τ_{xx} and τ_{xy} while both depend linearly on the Reynolds and the Weissenberg numbers.

With the aid of Eqs. (24), (79) and (80), the volumetric flow-rate, $Q(x) \equiv \int_0^1 u_x(x, y)dy$, is given by:

$$Q(x) = 1 - \varepsilon(1-x) + \varepsilon^2\left[-\frac{2\alpha^2}{15} + \left(-\frac{18}{35}\alpha\,\mathrm{Re} + \frac{14}{5}\mathrm{We}\,\eta_p\right)(1-x) + \frac{3}{2}(1-x)^2\right] + O(\varepsilon^3) \tag{89}$$

At $x = 0$, the above expression gives

$$Q(0) \approx 1 - \varepsilon + c\varepsilon^2 \tag{90}$$

where

$$c \equiv \frac{3}{2} - \frac{2\alpha^2}{15} - \frac{18}{35}\alpha\,\mathrm{Re} + \frac{14}{5}\mathrm{We}\,\eta_p > 0 \tag{91}$$

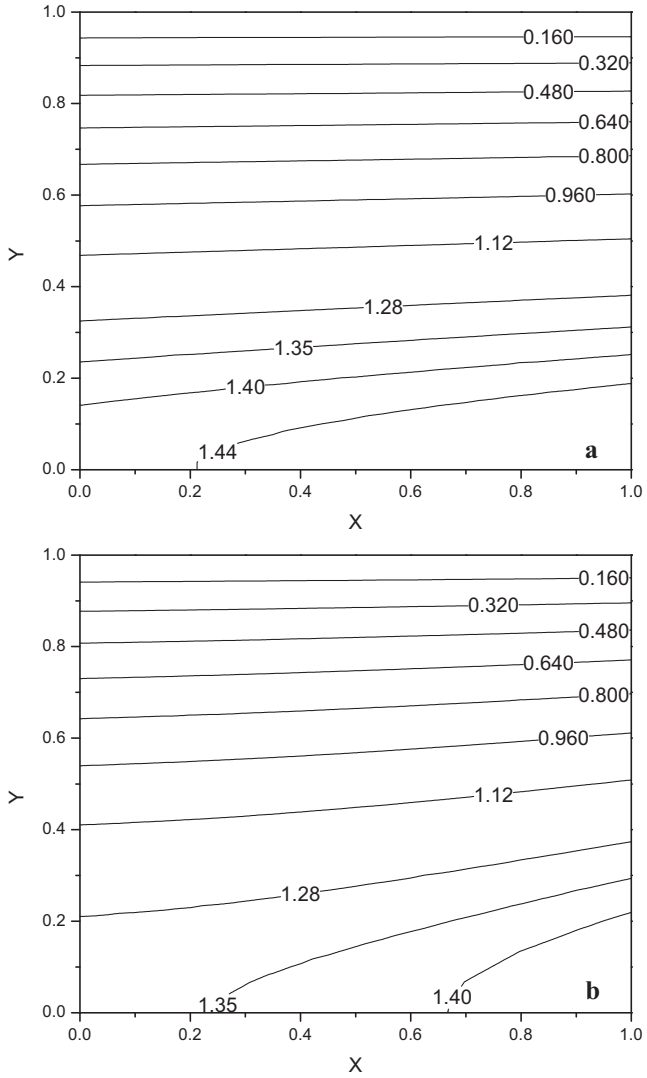

Fig. 6. Axial velocity field contours for We = 0.4, $\alpha = 0.01$, $\eta_s = 1/9$, and Re = 1: (a) $\varepsilon = 0.05$ and (b) $\varepsilon = 0.2$.

Hence, $Q(0)$ is a parabola with the minimum at $\varepsilon_c = 1/(2c)$. Since increasing ε must lead to more compression, i.e. to lower value at $Q(0)$ (in dimensional units), the perturbation solution is valid only when $\varepsilon < \varepsilon_c$. Similar conclusions have been reported for the Newtonian Poiseuille flows in capillaries [23] and slits [21]. Expressions (90) and (91) reveal that the presence of viscoelasticity reduces ε_c, i.e. it reduces the upper limit of validity of the perturbation solution, while the presence of inertia has the opposite effect. Fig. 1 shows the volumetric flow rates at the inlet of the channel, $Q(0)$, as a function of the compressibility parameter, ε, for two Newtonian and two viscoelastic cases with $\eta_s = 1/9$ and $a = 0.1$. In the Newtonian cases the critical compressibility values are $\varepsilon_c = 0.51$ and $\varepsilon_c = 0.33$ with and without inertia, respectively. The corresponding values in the viscoelastic cases are $\varepsilon_c \approx 0.25$ and $\varepsilon_c \approx 0.20$. Note also, that the difference in the volumetric flow rate between the inlet and the outlet plane of the channel is

$$\Delta Q \equiv Q(1) - Q(0) \approx \varepsilon(1 - c\varepsilon) \tag{92}$$

In a similar fashion, we define the average pressure $\Pi(x) \equiv \int_0^1 p(x, y)dy$, which, by virtue of Eqs. (24) and (78), is

$$\Pi(x) = (1-x) - \varepsilon\left[-\frac{a^2}{9} + \frac{(1-x)^2}{2} + \left(-\frac{18}{35}a\,\mathrm{Re} + \frac{14}{5}\eta_p \mathrm{We}\right)(1-x)\right] + \varepsilon^2\left[\frac{(1-x)^3}{2} - \frac{5}{3}a^2(1-x) - \frac{36}{35}a\,\mathrm{Re}(1-x)^2 + a\,\mathrm{Re}\left(\frac{2}{35}a^2 + \frac{3044}{13,475}a\,\mathrm{Re}(1-x)\right) + \eta_p\,\mathrm{We}\left\{-\frac{2}{45}a^2 + \left(-\frac{1478}{525}a\,\mathrm{Re} + \frac{\mathrm{We}}{175}(3316 - 2356\eta_s)\right)(1-x) + 7(1-x)^2\right\}\right] + O(\varepsilon^3) \tag{93}$$

Thus, the pressure difference between the entrance and the exit of the channel up to second order is found to be:

$$\Delta\Pi \equiv \Pi(0) - \Pi(1) \approx 1 - \varepsilon\left(\frac{1}{2} - \frac{18}{35}\alpha\,\mathrm{Re} + \frac{14}{5}\eta_p\,\mathrm{We}\right) + \varepsilon^2\left(\frac{1}{2} - \frac{5}{3}\alpha^2 - \frac{36}{35}\alpha\,\mathrm{Re} + \frac{3044}{13,475}\alpha^2\,\mathrm{Re}^2\right) + \varepsilon^2\eta_p\,\mathrm{We}\left[7 - \frac{1478}{525}\alpha\,\mathrm{Re} + \frac{\mathrm{We}}{175}(3316 - 2356\eta_s)\right] \tag{94}$$

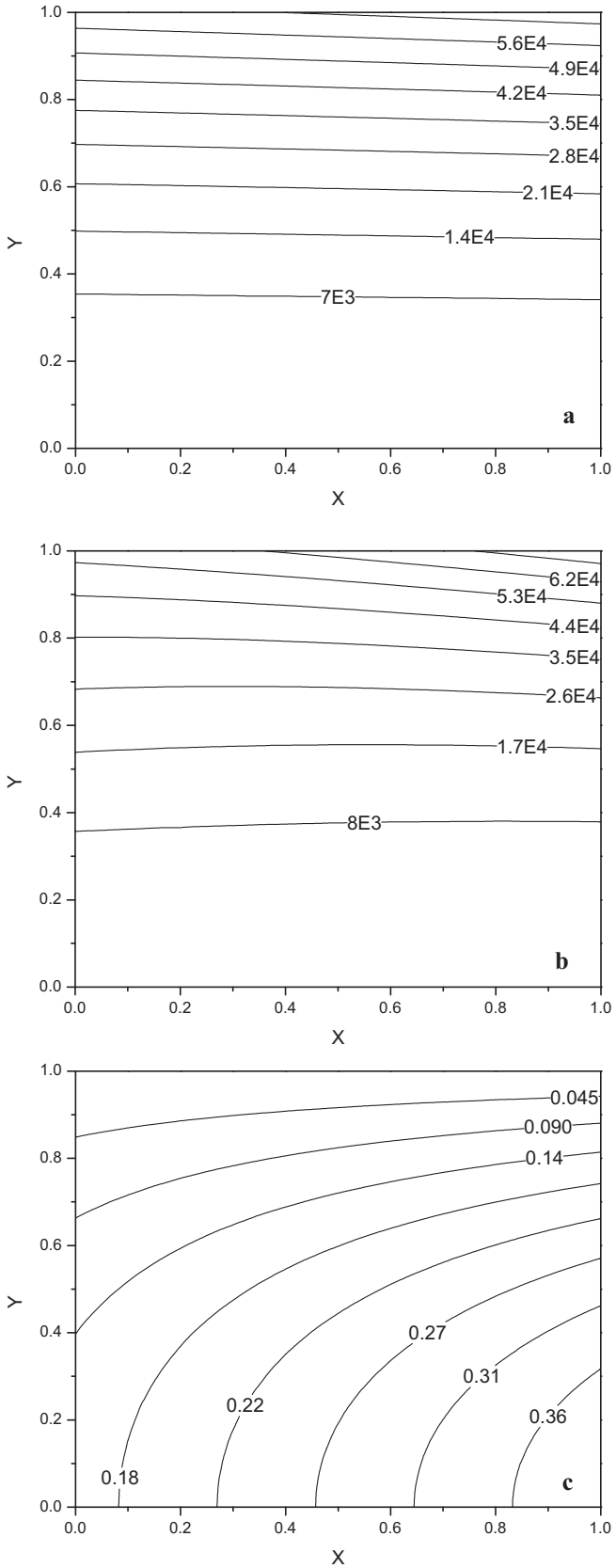

Fig. 7. Contours of extra stress component $S_{xx} = \eta_s \dot{\gamma}_{xx} + \eta_p \tau_{xx}$ for $\alpha = 0.01$, $\eta_s = 1/9$, and Re = 1: (a) We = 0.4, $\varepsilon = 0.05$; (b) We = 0.4, $\varepsilon = 0.2$; and (c) We = 0, $\varepsilon = 0.2$.

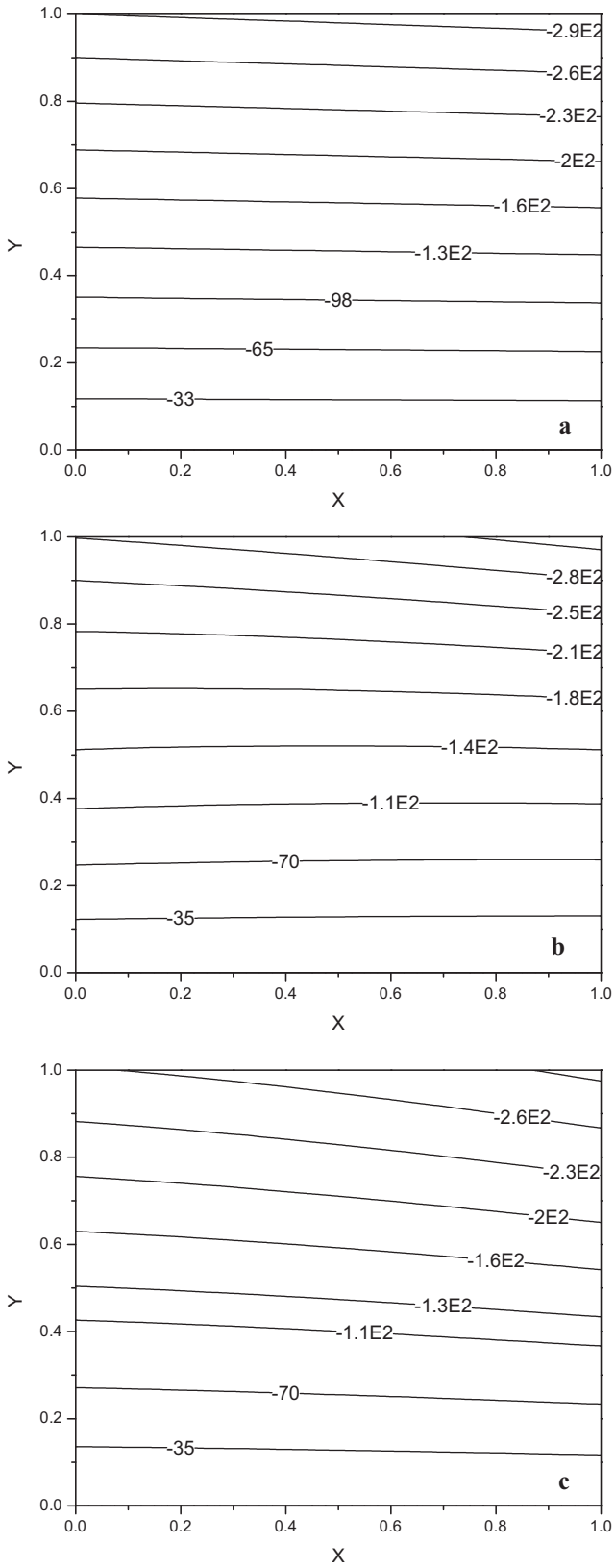

Fig. 8. Contours of extra stress component $S_{xy} = \eta_s \dot{\gamma}_{xy} + \eta_p \tau_{xy}$ for $\alpha = 0.01$, $\eta_s = 1/9$, and Re = 1: (a) We = 0.4, $\varepsilon = 0.05$; (b) We = 0.4, $\varepsilon = 0.2$; and (c) We = 0, $\varepsilon = 0.2$.

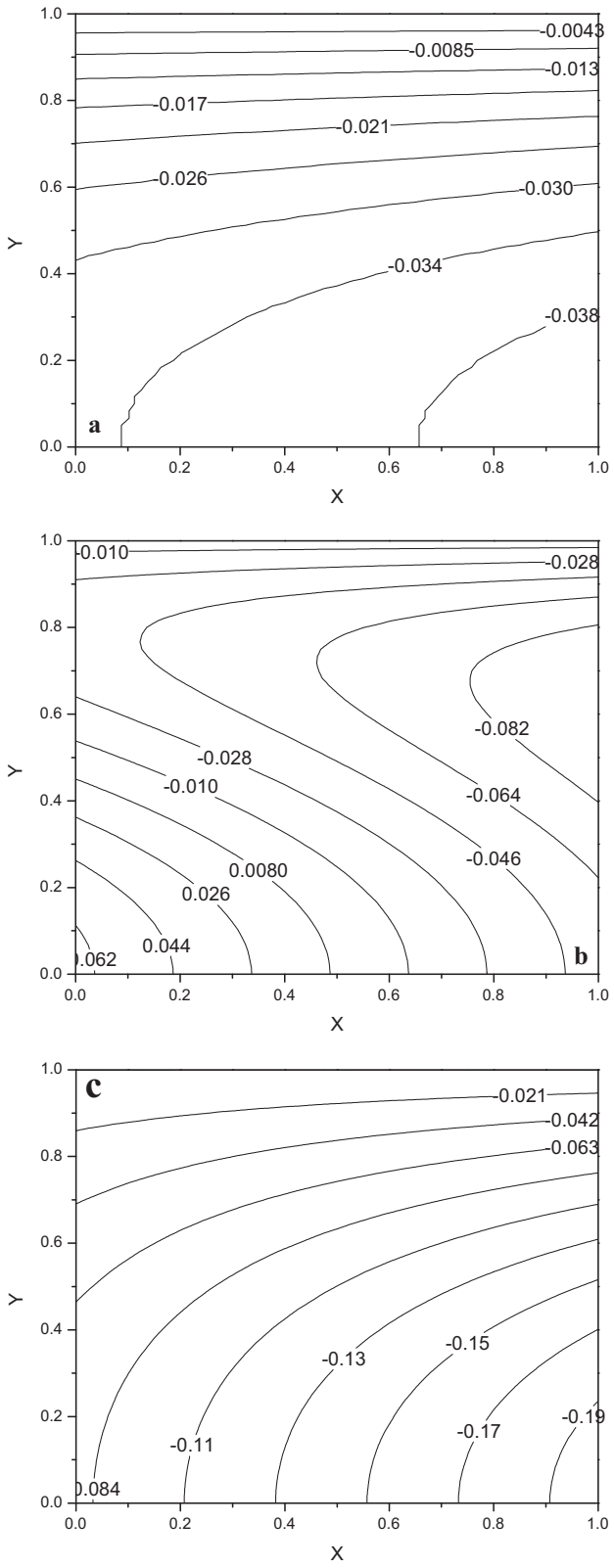

Fig. 9. Contours of extra stress component $S_{yy} = \eta_s \dot{\gamma}_{yy} + \eta_p \tau_{yy}$ for $\alpha = 0.01$, $\eta_s = 1/9$, and Re = 1: (a) We = 0.4, $\varepsilon = 0.05$; (b) We = 0.4, $\varepsilon = 0.2$; and (c) We = 0, $\varepsilon = 0.2$.

For We = 0, Eq. (94) reduces to the result of Venerus and Bugajsky [24] for a compressible Newtonian fluid with zero bulk viscosity. In Fig. 2, we plot the dimensionless flow curves, i.e. plots of the volumetric flow rate at the entrance of the channel versus the pressure drop, constructed by varying the compressibility number ε from $\varepsilon = 0$ to $\varepsilon = \varepsilon_c$ (the upper limit of validity of the perturbation solution) and calculating $Q(0)$ and $\Delta\Pi$ from Eqs. (90) and (94), respectively. For the Newtonian fluid (We = 0) and the weakly viscoelastic fluid (We = 0.1) it is seen that the flow curves are monotonic. However, as the Weissenberg number increases (We = 0.2 and 0.4) there is a range of $\Delta\Pi$ for which two solutions for $Q(0)$ are admissible.

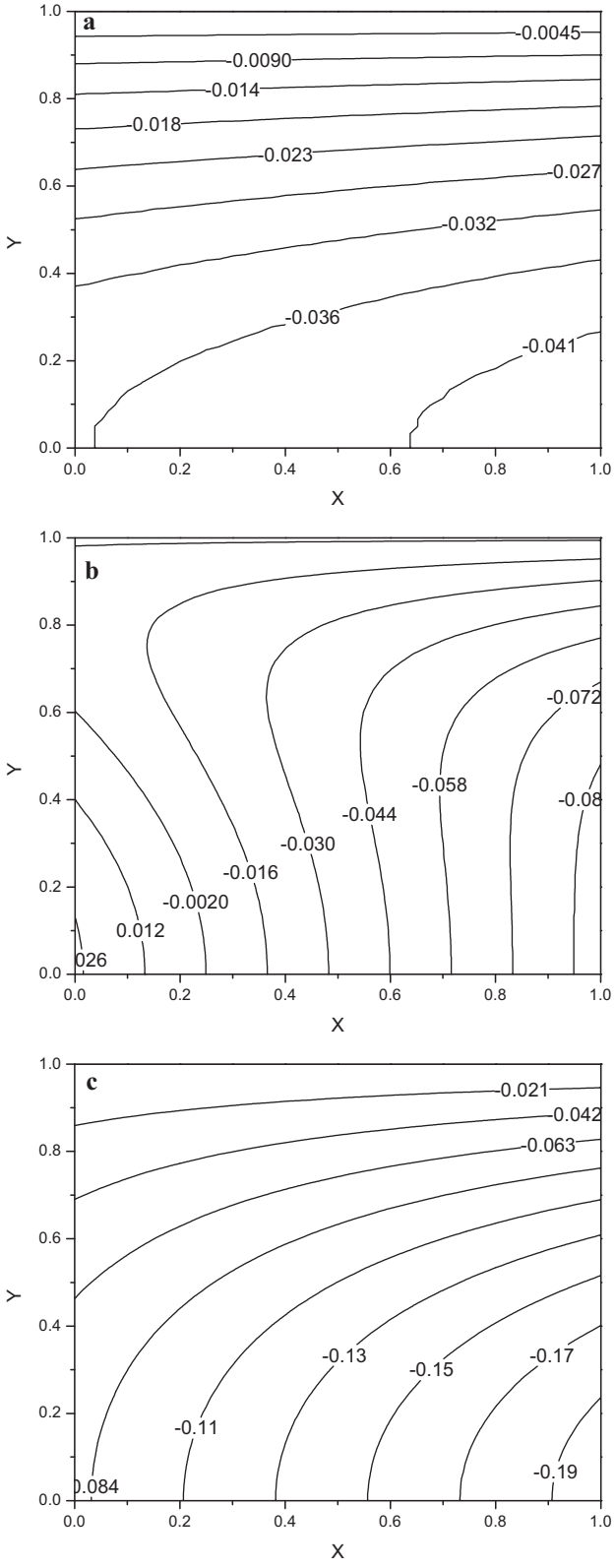

Fig. 10. Contours of extra stress component $S_{zz} = \eta_s \dot{\gamma}_{zz} + \eta_p \tau_{zz}$ for $\alpha = 0.01$, $\eta_s = 1/9$, and Re = 1: (a) We = 0.4, $\varepsilon = 0.05$; (b) We = 0.4, $\varepsilon = 0.2$; and (c) We = 0, $\varepsilon = 0.2$.

Let us now discuss in more detail the effects of the Weissenberg number and compressibility by fixing the values of the solvent viscosity ratio $\eta_s = 1/9$, $\eta_p = 8/9$, the aspect ratio to $\alpha = 0.01$, and the Reynolds number to Re = 1. The effect of the Weissenberg number on the streamwise and the normal velocity components is shown in Fig. 3. In particular, Fig. 3a illustrates the deviation of the streamwise velocity component from the incompressible (parabolic) profile near the channel exit ($x = 0.9$) for $\varepsilon = 0.2$ and various Weissenberg numbers (We = 0, 0.1, 0.2, and 0.4). The value of the compressibility parameter is actually the upper limit of validity of the perturbation solution (for We = 0.4 and Re = 1, $\varepsilon_c \approx 0.201$). It is seen that the effect of viscoelasticity decreases as we move away from the midplane center and diminishes at

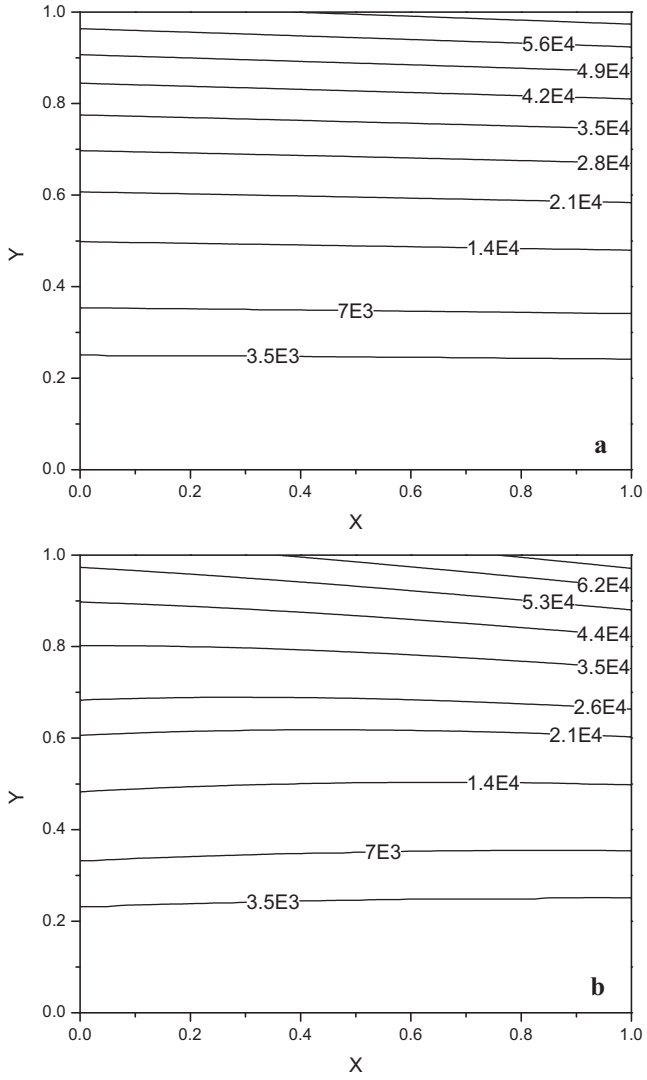

Fig. 11. Contours of the first normal stress difference, N_1, for We = 0.4, $\alpha = 0.01$, $\eta_s = 1/9$ and Re = 1: (a) $\varepsilon = 0.05$ and (b) $\varepsilon = 0.2$.

the wall. A similar behavior has also been observed for the effect of Reynolds number on the streamwise velocity [21]. The effect of the Weissenberg number on the transverse velocity component, which is an odd function of y, is illustrated in Fig. 3b. As implied by Eq. (81), this velocity component varies linearly with the Weissenberg number.

The effect of the compressibility parameter on the velocity components near the exit of the channel, $x = 0.9$, is illustrated in Fig. 4. As the compressibility parameter increases, the deviation of the streamwise velocity from the incompressible profile also increases. As pointed out earlier, this deviation is reduced from the midplane to the wall. As dictated by Eq. (81), u_y increases quadratically with ε.

In Fig. 5 the pressure contours for We = 0.4 and two values of the compressibility parameter, $\varepsilon = 0.05$ and 0.2, are shown. It should be noted that in both cases $\varepsilon^2\alpha^2/6 \ll 1$ while $\varepsilon_c \approx 0.201$. Also, the Reynolds numbers is set equal to 1 (and the same holds for Figs. 6–11). It is seen that the contours are similar, almost vertical and equidistant, and slightly shifted towards the exit of the channel. This is due to the fact that y-dependent terms are multiplied by the aspect ratio (see Eq. (78)), which in the present case is a very small. More pronounced differences are observed, however, in the axial velocity contours. As illustrated in Fig. 6, the contours of u_x, which are parallel everywhere in the case of incompressible flow and near the exit of the channel otherwise, are curved upstream towards the midplane. This is obviously due to the fact that for the mass to be preserved the flow accelerates downstream to counterbalance the reduction of the density.

In Figs. 7–10, we plotted the contours of the four non-trivial components of the extra stress tensor,

$$\underline{\underline{S}} = \eta_s \underline{\underline{\dot{\gamma}}} + \eta_p \underline{\underline{\tau}} \tag{95}$$

(i.e. of S_{xx}, S_{xy}, S_{yy}, and S_{zz}) for three different combinations of We and ε: (a) We = 0.4, $\varepsilon = 0.05$; (b) We = 0.4, $\varepsilon = 0.2$; and (c) We = 0, $\varepsilon = 0.2$. For We = 0 (Newtonian flow) S_{xx} is a strong function of ε and the transverse coordinate y. This dependence becomes weaker by increasing the value of the Weissenberg number and the contours of S_{xx} are almost horizontal. The effect of compressibility on S_{xy} appears to be weak. Nevertheless, it is clear from Fig. 8 that compressibility causes more rapid changes of S_{xy} near the wall. The effects are more dramatic on the other two extra stress components, provided that We is sufficiently high. For a given value of x, the values of S_{yy} in Fig. 9b (We = 0.4, $\varepsilon = 0.2$) pass through a minimum as y is increased from 0 to 1. A similar trend is observed for S_{zz} in Fig. 10b.

Finally, the contours for the first normal stress difference, $N_1 \equiv S_{xx} - S_{yy}$, for We = 0.4 and $\varepsilon = 0.05$ and 0.2 are presented in Fig. 11. These follow the same pattern as those of S_{xx}, which is expected, since S_{xx} dominates S_{yy}. The second normal stress difference, $N_2 \equiv S_{yy} - S_{zz}$, is non-zero but very small. Even for highly viscoelastic liquids, its values are of the order of 10^{-4}.

5. Conclusions

A perturbation solution for the laminar, isothermal, weakly compressible plane Poiseuille flow of an Oldroyd-B fluid has been derived. The primary variables of the flow, namely the velocity, pressure, mass density and polymer extra-stress fields, are expanded as power series of the compressibility number and the solution is obtained up to second-order. Expressions for the volumetric flow and the pressure drop between the entrance and the exit of the channel, up to second-order, are also derived. It is demonstrated that fluid compressibility, inertia and viscoelasticity have a significant effect on the transverse velocity component, the extra stress tensor, and the first normal difference.

Appendix A. Extra stress components of the constitutive equation

From the zero-, first- and second-order terms of the constitutive model, one gets a first-order differential equation of the form:

$$\mathrm{We}\, u_{x0} \frac{\partial \tau_k}{\partial x} + \tau_k = m_k, \tag{A1}$$

where u_{x0} is a function of y, given by Eq. (25), τ_k is the k-order contribution to any stress component and m_k is a known function, which for the three cases of interest is given by:

$$\left.\begin{array}{l} m_0(y) = C_0(y) \\ m_1(x,y) = B_1(y)x + C_1(y) \\ m_2(x,y) = A_2(y)x^2 + B_2(y)x + C_2(y) \end{array}\right\} \tag{A2}$$

The general solution of (A1) is:

$$\tau_k = K(y) e^{-(x/\mathrm{We}\, u_{x0})} + \frac{1}{\mathrm{We}\, u_{x0}} e^{-(x/\mathrm{We}\, u_{x0})} \int m_k e^{x/\mathrm{We}\, u_{x0}} dx \tag{A3}$$

However, for a continuous dependence of the solution on the Weissenberg number, we set $K = 0$. In addition, substituting (A2) into (A3) and integrating by parts, we get:

$$\tau_k = \left(\mathrm{We}^2 u_{x0}^2 - \mathrm{We}\, u_{x0} x + \frac{1}{2}x^2\right) \frac{\partial^2 m_k}{\partial x^2} + (x - \mathrm{We}\, u_{x0}) \frac{\partial m_k}{\partial x}(0,y) + m_k(0,y) \tag{A4}$$

The above solution for the three cases of interest is simplified as follows:

$$\left.\begin{array}{l} \tau_0 = C_0(y) \\ \tau_1 = (x - \mathrm{We}\, u_{x0}) B_1(y) + C_1(y) \\ \tau_2 = 2(\mathrm{We}^2 u_{x0}^2 - \mathrm{We}\, u_{x0} x + x^2/2) A_2(y) + (x - \mathrm{We}\, u_{x0}) B_2(y) + C_2(y) \end{array}\right\} \tag{A5}$$

References

[1] S.G. Hatzikiriakos, J.M. Dealy, Role of slip and fracture in the oscillating flow of HDPE in a capillary, J. Rheol. 36 (1992) 845–884.
[2] I.J. Keshtiban, F. Belblidia, M.F. Webster, Computation of incompressible and weakly-compressible viscoelastic liquids flow: finite element/volume schemes, J. Non-Newtonian Fluid Mech. 126 (2005) 123–143.
[3] G. Vinay, A. Wachs, I. Frigaard, Numerical simulation of weakly compressible Bingham flows: the restart of pipeline flows of waxy crude oils, J. Non-Newtonian Fluid Mech. 136 (2006) 93–105.
[4] C. Guillopé, A. Hakim, R. Talhouk, Existence of steady flows of slightly compressible viscoelastic fluids of White-Metzner type around an obstacle, Commun. Pure Appl. Anal. 4 (2005) 23–43.
[5] E. Taliadorou, G. Georgiou, A.N. Alexandrou, A two-dimensional numerical study of the stick-slip extrusion instability, J. Non-Newtonian Fluid Mech. 146 (2007) 30–44.
[6] G.C. Georgiou, M.J. Crochet, Compressible viscous flow in slits with slip at the wall, J. Rheol. 38 (1994) 639–654.
[7] E. Taliadorou, G.C. Georgiou, E. Mitsoulis, Numerical simulation of the extrusion of strongly compressible Newtonian liquids, Rheol. Acta 47 (2008) 49–62.
[8] S.G. Hatzikiriakos, J.M. Dealy, Start-up pressure gradients in a capillary rheometer, Polym. Eng. Sci. 34 (1994) 493–499.
[9] M. Ranganathan, M.R. Mackley, P.H.J. Spitteler, The application of the multipass rheometer to time-dependent capillary flow measurements of a polyethylene melt, J. Rheol. 43 (1999) 443–451.
[10] V. Valério, M.S. Carvalho, C. Tomei, Efficient computation of the spectrum of viscoelastic flows, J. Comp. Phys. 228 (2009) 1172–1187.
[11] G. Georgiou, The time-dependent, compressible Poiseuille and extrudate-swell flows of a Carreau fluid with slip at the wall, J. Non-Newtonian Fluid Mech. 109 (2003) 93–114.
[12] R. Valette, M.R. Mackley, G. Hernandez Fernandez del Castillo, Matching time dependent pressure driven flows with a Rolie Poly numerical simulation, J. Non-Newtonian Fluid Mech. 136 (2006) 118–125.
[13] E. Mitsoulis, O. Delgadillo-Velazquez, S.G. Hatzikiriakos, Transient capillary-rheometry: compressibility effects, J. Non-Newtonian Fluid Mech. 145 (2007) 102–108.
[14] E. Taliadorou, G.C. Georgiou, I. Moulitsas, Weakly compressible Poiseuille flows of a Herschel-Bulkley fluid, J. Non-Newtonian Fluid Mech. 158 (2009) 162–169.
[15] I.J. Keshtiban, F. Belblidia, M.F. Webster, Numerical simulation of compressible viscoelastic liquids, J. Non-Newtonian Fluid Mech. 122 (2004) 131–146.
[16] E.A. Brujan, A first-order model for bubble dynamics in a compressible viscoelastic fluid, J. Non-Newtonian Fluid Mech. 84 (1999) 83–103.
[17] F. Belblidia, I.J. Keshtiban, M.F. Webster, Stabilised computations for viscoelastic flows under compressible considerations, J. Non-Newtonian Fluid Mech. 134 (2006) 56–76.
[18] B. Puangkird, F. Belblidia, M.F. Webster, Numerical simulation of viscoelastic fluids in cross-slot devices, J. Non-Newtonian Fluid Mech. 162 (2009) 1–20.
[19] B.J. Edwards, A.N. Beris, Remarks concerning compressible viscoelastic fluid models, J. Non-Newtonian Fluid Mech. 36 (1990) 411–417.
[20] S. Matusu-Necasova, A. Sequeira, J.H. Videman, Existence of classical solutions for compressible viscoelastic fluids of Oldroyd type past an obstacle, Math. Methods Appl. Sci. 22 (1999) 449–460.
[21] E.G. Taliadorou, M. Neophytou, G.C. Georgiou, Perturbation solutions of Poiseuille flows of weakly compressible Newtonian liquids, J. Non-Newtonian Fluid Mech. 158 (2009) 162–169.

[22] S. Joseph, L. Joseph, G.C. Georgiou, Perturbation solution of the compressible annular Poiseuille flow of a viscous fluid, J. Non-Newtonian Fluid Mech. 165 (2010) 676–680.
[23] D.C. Venerus, Laminar capillary flow of compressible viscous fluids, J. Fluid Mech. 555 (2006) 59–80.
[24] D.C. Venerus, D.J. Bugajsky, Compressible laminar flow in a channel, Phys. Fluids 22 (2010) 046101.
[25] Wolfram Research, Inc., Mathematica Edition: Version 7.0, Wolfram Research, Inc., Champaign, Illinois, 2008.
[26] T. Poinsot, S. Lele, Boundary conditions for direct simulations of compressible viscous flows, J. Comp. Phys. 101 (1992) 104–129.
[27] L.W. Schwartz, A perturbation solution for compressible viscous channel flows, J. Eng. Math. 21 (1987) 69–86.